



NRC Publications Archive Archives des publications du CNRC

Application of Ultrasound and Neural Networks in the Determination of Filler Concentration and Dispersion during Polymer Extrusion Processes

Sun, Zhigang; Jen, Cheng-Kuei; Yan, Jian; Chen, Ming-Yuan

This publication could be one of several versions: author's original, accepted manuscript or the publisher's version. / La version de cette publication peut être l'une des suivantes : la version prépublication de l'auteur, la version acceptée du manuscrit ou la version de l'éditeur.

For the publisher's version, please access the DOI link below. / Pour consulter la version de l'éditeur, utilisez le lien DOI ci-dessous.

Publisher's version / Version de l'éditeur:

<https://doi.org/10.1002/pen.20328>

Polymer Engineering and Science, 45, 6, pp. 764-772, 2005-06-01

NRC Publications Record / Notice d'Archives des publications de CNRC:

<https://nrc-publications.canada.ca/eng/view/object/?id=be4c3298-a894-422a-a5ac-7fea9a29f13f>

<https://publications-cnrc.canada.ca/fra/voir/objet/?id=be4c3298-a894-422a-a5ac-7fea9a29f13f>

Access and use of this website and the material on it are subject to the Terms and Conditions set forth at

<https://nrc-publications.canada.ca/eng/copyright>

READ THESE TERMS AND CONDITIONS CAREFULLY BEFORE USING THIS WEBSITE.

L'accès à ce site Web et l'utilisation de son contenu sont assujettis aux conditions présentées dans le site

<https://publications-cnrc.canada.ca/fra/droits>

LISEZ CES CONDITIONS ATTENTIVEMENT AVANT D'UTILISER CE SITE WEB.

Questions? Contact the NRC Publications Archive team at

PublicationsArchive-ArchivesPublications@nrc-cnrc.gc.ca. If you wish to email the authors directly, please see the first page of the publication for their contact information.

Vous avez des questions? Nous pouvons vous aider. Pour communiquer directement avec un auteur, consultez la première page de la revue dans laquelle son article a été publié afin de trouver ses coordonnées. Si vous n'arrivez pas à les repérer, communiquez avec nous à PublicationsArchive-ArchivesPublications@nrc-cnrc.gc.ca.



Application of Ultrasound and Neural Networks in the Determination of Filler Dispersion During Polymer Extrusion Processes

Zhigang Sun, Cheng-Kuei Jen

Industrial Materials Institute, National Research Council, 75 de Mortagne Blvd., Boucherville, Quebec J4B 6Y4, Canada

Jian Yan, Ming-Yuan Chen

Mechanical and Industrial Engineering Department, Concordia University, 1455 de Maisonneuve Blvd. W., Montreal, Quebec H3G 1M8, Canada

Mineral filler dispersion is important information for the production of mineral-charged polymers. In order to achieve timely control of product quality, a technique capable of providing real-time information on filler dispersion is highly desirable. In this work, ultrasound, temperature, and pressure sensors as well as an amperemeter of the extruder motor drive were used to monitor the extrusion of mineral-filled polymers under various experimental conditions in terms of filler type, filler concentration, feeding rate, screw rotation speed, and barrel temperature. Then, neural network relationships were established among the filler dispersion index and three categories of variables, namely, control variables of the extruder, extruder-dependent measured variables, and extruder-independent measured variables (based on ultrasonic measurement). Of the three categories of variables, the process control variables and extruder-independent ultrasonically measured variables performed best in inferring the dispersion index through a neural network model. While the neural network model based on control variables could help determine the optimal experimental conditions to achieve a dispersion index, the extruder-independent network model based on ultrasonic measurement is suitable for in-line measurement of the quality of dispersion. This study has demonstrated the feasibility of using ultrasound and neural networks for in-line monitoring of dispersion during extrusion processes of mineral-charged polymers. *POLYM. ENG. SCI.*, 45:764–772, 2005. © 2005 Society of Plastics Engineers

INTRODUCTION

Mineral-reinforced polymers are widely used in today's industries for their improved mechanical properties in comparison with nonreinforced ones. Mineral filler dispersion is an important factor affecting the properties of the filled polymers. In order to achieve timely control of product quality, a technique capable of providing real-time information on filler concentration and dispersion during the fabrication of mineral-filled polymers is highly desirable. Optical microscopy and scanning electron microscopy (SEM) are two of the most widely used techniques for evaluating the quality of filler dispersion [1–3]. Other techniques include electrical conductivity and dielectric measurements [4], nuclear magnetic resonance (NMR) [5], and X-ray scattering analysis [6]. All the methods mentioned above are time consuming and cannot be used on-line to meet the need of real-time control of the quality of manufactured products.

Ultrasound is one of the popular means for industrial process monitoring and material characterization, owing to its robustness, fast response, nondestructiveness, noninvasiveness, and cost-effectiveness. As far as mineral-reinforced polymer processing is concerned, ultrasound is sensitive to mineral filler concentration and the dispersion condition of the filler in the molten polymer matrix [7–9]. This sensitivity makes it possible to use ultrasound to determine filler concentration and dispersion. However, the ultrasonic properties (i.e., ultrasound velocity and attenuation) of a mineral-filled polymer depend not only on the filler concentration and dispersion, but also on melt temperature, pressure, molecular weight, and the shear rate of the melt. If an explicit relationship between the ultrasonic properties, filler dispersion, and other intervening factors were known, it would be trivial to determine the filler dispersion through this relationship and ultrasonic measurements.

Correspondence to: Z. Sun; e-mail: zhigang.sun@cnrc-nrc.gc.ca
Contract grant sponsor: Natural Sciences and Engineering Research Council of Canada (NSERC).
DOI 10.1002/pen.20328
Published online in Wiley InterScience (www.interscience.wiley.com).
© 2005 Society of Plastics Engineers

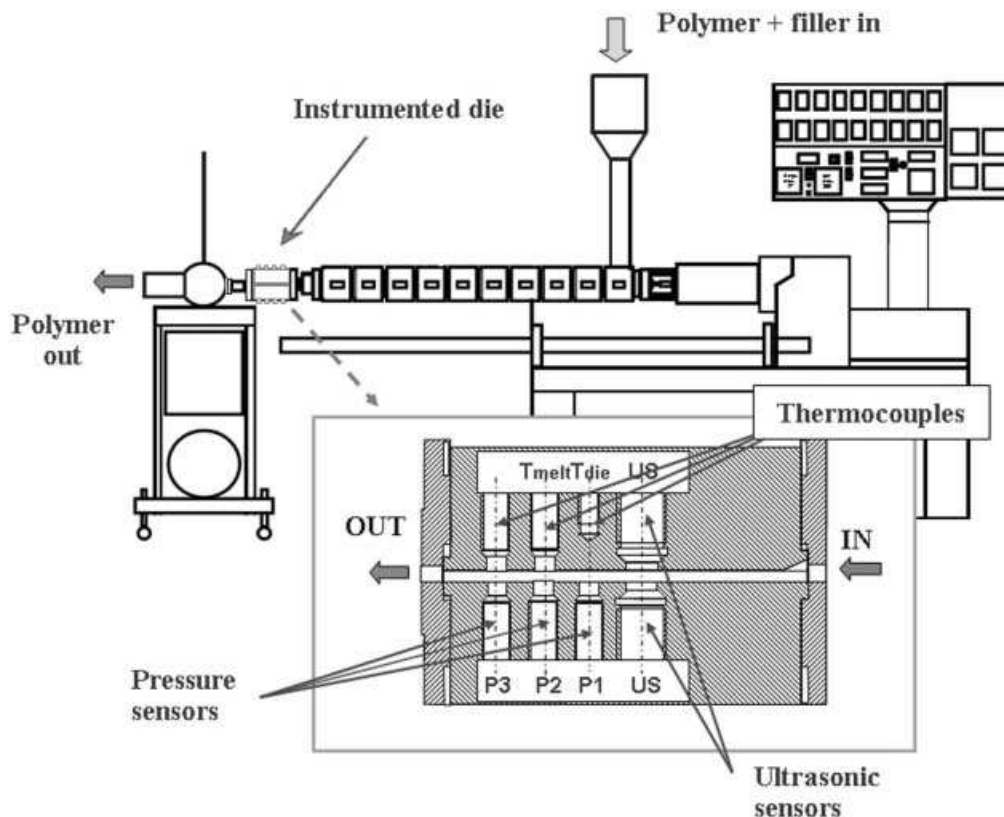


FIG. 1. Schematic of the extruder and instrumented die used in the experiments. The locations of three pressure sensors in the instrumented are indicated with P_1 , P_2 , and P_3 . The ultrasonic sensors are indicated with US, and the melt thermocouple is indicated with T_{melt} .

However, at the current state of the art, such an explicit relationship cannot be established easily, due to the lack of thorough understanding of the interaction between ultrasound and filled polymers under flowing condition.

Artificial neural networks provide a way for modeling the relationship among measured and controlled parameters of a complex process without the need of thorough understanding of the process itself [10]. There has been work on the use of neural networks and ultrasound for quantifying the dispersion of mineral filler in a polymer [11]. The current work is a continuation of the work carried out earlier at our institute and presented in Ref. 11, and constitutes one of our steps toward establishing a way of using ultrasound for online determination of filler dispersion state. In this work, attempts have been made to build neural networks that relate the filler dispersion index to each of three categories of variables, namely, control variables of the extruder, extruder-dependent measured variables, and extruder-independent measured variables based on ultrasonic measurement. The purpose is to show, through example networks, that a combination of ultrasonic measurement and neural networks could be a viable approach to in-line determination of filler dispersion index. Although the structure and training algorithm of a network can have crucial impact on the performance of the network, we will focus on more fundamental issues such as selections of input variables for

filler dispersion monitoring, and the physical reasons behind these choices and their consequences, rather than on pure technical issues as to how a network should be structured and trained. That being said, and keeping in mind that there are numerous ways to design the architecture of a neural network and there are various ways to do the training, the network presented in this work is by no means intended to be the best performing one, but rather one that performs reasonably well. The readers can certainly build their own neural networks by respecting some of the considerations discussed in this article.

EXPERIMENTS

Polypropylene (PP) 6631 from Himont Canada, with density $\rho = 890 \text{ kg/m}^3$ and melt flow rate (MFR) = 2.0 dg/min, was used in this study. Two grades of calcium carbonate powders, Camel-Cal and Camel-Cal-ST, supplied by Genstar, with specific gravity of 2.71 were used as fillers. Both grades had a mean particle size of $0.7 \mu\text{m}$, with 90% of the particles finer than $2 \mu\text{m}$, and 100% finer than $7 \mu\text{m}$. The grade with suffix ST was stearate-coated to allow for better particle dispersion.

A Leistritz 34-mm corotating intermeshing twin-screw extruder, composed of 12 barrel sections with a barrel-length-to-diameter ratio (L/D) of 42, was used. Polyprop-

TABLE 1. Experimental data.*

Sample index	F_{type}	C_f (%)	T_{prfl}	V_{RPM} (RPM)	Q_{Feed} (kg/h)	V_{us} (m/s)	α_{us} (dB/cm)	A_{mps} (A)	T_{meit} (°C)	P_1 (MPa)	P_2 (MPa)	P_3 (MPa)	P_{us} (MPa)	D_x
1	Non_ST	15	1	100	8.8235	886.71	17.096	26.48	231.36	2.7618	1.8339	0.9636	3.7362	0.6906
2	Non_ST	10	1	300	8.3333	845.26	15.636	18.679	233.25	2.3071	1.5397	0.8203	3.1129	0.7085
3	Non_ST	20	2	300	9.375	863.12	18.901	20.343	212.06	2.8641	1.9170	1.0038	3.8587	0.7623
4	Non_ST	15	1	175	8.8235	865.96	15.763	22.228	232.05	2.6226	1.7405	0.9160	3.5489	0.7635
5	Non_ST	5	2	100	7.8947	942.02	6.5622	24.082	204.73	2.8826	1.9427	1.0182	3.8695	0.7763
6	Non_ST	5	1	100	7.8947	899.16	7.628	23.113	231.07	2.4695	1.6415	0.8741	3.339	0.7802
7	Non_ST	15	2	300	8.8235	872.49	16.238	19.487	210.27	2.7163	1.8206	0.9592	3.6567	0.7864
8	Non_ST	20	2	100	4.375	921.8	14.964	18.758	205.66	2.5777	1.7353	0.9013	3.4623	0.7976
9	Non_ST	20	1	175	4.375	851.05	17.808	16.75	230.75	2.0531	1.3570	0.7105	2.7842	0.8
10	Non_ST	5	2	100	3.6842	945.68	6.3547	15.718	205.37	2.2566	1.5214	0.7991	3.0286	0.8093
11	Non_ST	20	1	300	4.375	825.03	20.586	15.603	232.3	1.9411	1.2926	0.6814	2.6222	0.8115
12	Non_ST	10	2	100	3.8889	937.15	8.8756	16.579	205.42	2.3407	1.5776	0.8269	3.1421	0.8196
13	Non_ST	20	2	175	4.375	896.66	15.265	17.557	207.26	2.4783	1.6652	0.8632	3.3322	0.8254
14	Non_ST	15	1	100	4.1176	881.97	15.125	17.353	230.57	2.0424	1.3503	0.7139	2.7693	0.827
15	Non_ST	20	2	300	4.375	859.95	18.29	15.463	209.14	2.1764	1.4534	0.7636	2.9357	0.8283
16	Non_ST	15	2	175	4.1176	903.88	12.901	16.677	206.75	2.3535	1.5854	0.8289	3.16	0.8331
17	Non_ST	5	1	300	3.6842	851.39	8.7336	13.323	230.6	1.5441	1.0323	0.5581	2.0815	0.8498
18	Non_ST	5	1	175	3.6842	879.97	8.1665	13.912	230.65	1.7764	1.1864	0.6380	2.396	0.8517
19	Non_ST	10	2	300	3.8889	877.86	11.66	13.988	204.82	1.9236	1.2907	0.6845	2.5882	0.8599
20	Non_ST	5	2	175	3.6842	919.95	7.4962	14.768	206.2	2.1121	1.4262	0.7497	2.8324	0.8632
21	Non_ST	10	1	300	3.8889	841.28	13.075	14.479	231.31	1.6806	1.1225	0.6029	2.2667	0.8754
22	ST	10	1	100	8.3333	890.77	10.826	23.155	230.21	2.3865	1.6746	0.9119	3.1341	0.7223
23	ST	15	1	100	8.8235	884.17	14.888	23.903	230.41	2.4850	1.7446	0.9440	3.2626	0.7543
24	ST	5	1	100	7.8947	897.08	6.5878	22.285	229.97	2.2826	1.6031	0.8772	2.9962	0.7809
25	ST	20	1	100	9.375	877.28	18.053	24.6	231.21	2.5719	1.8005	0.9671	3.3819	0.7829
26	ST	20	1	175	9.375	855.18	15.817	21.408	231.22	2.3470	1.6713	0.9044	3.0567	0.7909
27	ST	15	2	100	8.8235	921.48	11.479	22.931	205.28	2.7991	1.9826	1.0438	3.6565	0.8119
28	ST	10	1	175	8.3333	869.49	10.566	20.653	229.54	2.0577	1.5594	0.8567	2.581	0.8183
29	ST	5	2	300	7.8947	882.6	10.336	19.854	204.76	2.2824	1.6121	0.8505	2.9863	0.8267
30	ST	15	1	300	8.8235	833.49	15.774	18.542	233.47	2.2280	1.5632	0.8474	2.9262	0.8368
31	ST	20	2	100	9.375	914.18	14.632	24.007	205.62	2.9091	2.0517	1.0808	3.8095	0.8371
32	ST	20	1	300	9.375	826.71	17.115	18.576	233.42	2.3022	1.6133	0.8703	3.0256	0.8445
33	ST	20	1	175	4.375	850.6	13.121	16.267	230.76	1.7504	1.2762	0.6570	2.2486	0.8482
34	ST	20	1	100	4.375	871.25	13.44	15.357	229.24	1.8510	1.3569	0.7268	2.3698	0.8531
35	ST	10	1	300	8.3333	842.03	13.642	18.933	232.97	2.1696	1.5248	0.8302	2.8468	0.8549
36	ST	10	2	100	8.3333	929.95	8.0875	22.098	204.88	2.6981	1.9144	1.0087	3.5212	0.8554
37	ST	10	2	300	3.8889	873.89	8.8515	13.923	205.41	1.7902	1.2790	0.6690	2.3271	0.8628
38	ST	5	1	175	3.6842	875.6	6.8962	14.714	230.3	1.5565	1.1469	0.5969	1.9866	0.864
39	ST	15	1	175	4.1176	858.51	10.984	15.519	230.68	1.6741	1.2251	0.6327	2.1456	0.8671
40	ST	15	2	175	4.1176	901.31	10.083	15.12	205.01	2.0562	1.4589	0.7596	2.6833	0.8678
41	ST	15	2	300	8.8235	864.57	13.88	20.396	208.34	2.4750	1.7439	0.9178	3.2428	0.8689
42	ST	20	2	300	4.375	855.23	13.196	14.679	206.29	1.9440	1.3830	0.7189	2.5334	0.8708
43	ST	15	1	100	4.1176	880.27	11.199	14.704	228.93	1.7819	1.3122	0.7075	2.275	0.872
44	ST	5	2	175	3.6842	920.38	6.6897	14.338	204.31	1.9353	1.3754	0.7171	2.5234	0.8735
45	ST	10	2	175	8.3333	908.79	8.3866	21.11	206.49	2.5726	1.8059	0.9471	3.3778	0.8812
46	ST	5	2	100	3.6842	942.93	5.5136	15.395	202.93	1.9904	1.4407	0.7597	2.5678	0.883
47	ST	10	1	300	3.8889	835	9.4031	14.917	231.23	1.4522	1.0699	0.5652	1.8538	0.903
48	Non_ST	10	1	100	8.3333	892.7	12.486	24.585	231.15	2.6153	1.7375	0.9200	3.537	0.6999
49	Non_ST	20	1	300	9.375	827.32	21.721	20.039	233.9	2.5553	1.6980	0.8895	3.4556	0.7499
50	Non_ST	5	1	300	7.8947	854.27	10.817	17.419	232.2	2.1360	1.4279	0.7636	2.8796	0.7605
51	Non_ST	20	1	175	9.375	857.94	19.462	23.264	232.54	2.7771	1.8374	0.9566	3.7639	0.7624
52	Non_ST	15	2	100	8.8235	928.54	14.553	27.405	206.26	3.1531	2.1248	1.1087	4.233	0.7772
53	Non_ST	10	2	100	8.3333	934.65	10.406	25.419	205.34	2.9989	2.0211	1.0575	4.0257	0.7809
54	Non_ST	20	2	175	9.375	892.57	17.649	24.538	206	3.1007	2.0864	1.0772	4.1659	0.7818
55	Non_ST	10	1	175	8.3333	873.26	12.158	21.319	231.65	2.4774	1.6463	0.8737	3.3502	0.7836
56	Non_ST	15	2	175	8.8235	900.75	13.946	23.306	204.88	2.9419	1.9843	1.0302	3.9475	0.7901
57	Non_ST	20	1	100	3.75	876.06	17.906	18.611	230.98	2.1980	1.4502	0.7615	2.9834	0.7938
58	Non_ST	15	1	300	8.8235	836.76	18.138	18.952	233.16	2.4028	1.6010	0.8467	3.2447	0.7989
59	Non_ST	5	2	300	7.8947	891.48	10.866	17.645	208.02	2.4438	1.6387	0.8689	3.2893	0.8036
60	Non_ST	5	1	175	7.8947	881.16	8.0002	20.179	231.25	2.3421	1.5571	0.8307	3.1664	0.811
61	Non_ST	5	2	300	3.5526	887.26	8.2033	13.243	206.43	1.7709	1.1889	0.6350	2.3821	0.8176
62	Non_ST	15	1	175	3.6765	857.84	14.832	15.971	229.76	1.9124	1.2680	0.6709	2.589	0.8189

TABLE 1. (Continued)

Sample index	F_{type}	C_f (%)	T_{prfl}	V_{RPM} (RPM)	Q_{Feed} (kg/h)	V_{us} (m/s)	α_{us} (dB/cm)	A_{mps} (A)	T_{melt} (°C)	P_1 (MPa)	P_2 (MPa)	P_3 (MPa)	P_{us} (MPa)	D_x
63	Non_ST	5	1	100	3.5526	897.02	7.3819	15.302	230.31	1.8628	1.2376	0.6641	2.5194	0.8254
64	Non_ST	5	2	175	7.8947	922.32	7.1746	20.16	206.24	2.7381	1.8343	0.9711	3.6873	0.8255
65	Non_ST	10	1	100	3.6111	889.66	11.388	16.213	230.52	1.9470	1.2924	0.6872	2.6345	0.8268
66	Non_ST	15	1	300	3.6765	833.03	17.094	14.952	231.73	1.7882	1.1924	0.6357	2.4137	0.834
67	Non_ST	10	2	175	8.3333	908.94	10.593	22.369	203.36	2.7942	1.8861	0.9829	3.7478	0.837
68	Non_ST	10	2	300	8.3333	881.56	13.98	18.821	209.24	2.5875	1.7349	0.9173	3.4828	0.845
69	Non_ST	15	2	100	3.6765	928.27	12.113	17.763	205.58	2.4565	1.6551	0.8643	3.298	0.8523
70	Non_ST	10	2	175	3.6111	911.3	10.061	15.566	206.43	2.2032	1.4871	0.7801	2.9551	0.8552
71	Non_ST	15	2	300	3.6765	868.29	14.433	14.632	206.3	2.0013	1.3390	0.7044	2.6968	0.8634
72	Non_ST	5	1	225	3.5526	866.41	8.4376	13.706	230.99	1.7439	1.1655	0.6271	2.3513	0.8676
73	ST	15	1	175	8.8235	862.27	13.474	21.237	230.16	2.2293	1.6247	0.8857	2.8641	0.7096
74	ST	5	1	175	7.8947	877.28	7.3736	20.332	228.55	2.0166	1.5000	0.8284	2.5592	0.776
75	ST	5	2	100	7.8947	939.46	5.3675	21.52	204.65	2.6470	1.8799	0.9911	3.4526	0.8119
76	ST	20	2	175	9.375	890.99	13.766	22.415	207.11	2.8086	1.9643	1.0266	3.6954	0.8274
77	ST	15	2	175	8.8235	900	10.766	21.696	206.73	2.6948	1.8884	0.9895	3.5416	0.8309
78	ST	20	2	100	3.75	912.72	12.233	16.285	204.22	2.1434	1.5438	0.8114	2.7731	0.8372
79	ST	5	1	100	3.5526	898.66	6.1621	13.973	228.68	1.6749	1.2401	0.6719	2.1316	0.8484
80	ST	10	2	300	8.3333	872.7	11.972	19.865	207.06	2.3828	1.6815	0.8874	3.1192	0.8513
81	ST	20	2	175	3.75	892.35	12.073	15.846	205.32	2.1299	1.5084	0.7828	2.7827	0.8532
82	ST	20	1	300	3.75	818.25	13.786	15.52	231.91	1.5704	1.1533	0.5964	2.0085	0.8574
83	ST	5	2	300	3.5526	883.42	6.8909	13.55	204.62	1.7405	1.2469	0.6563	2.2588	0.8602
84	ST	20	2	300	9.375	856.82	16.362	20.571	209.54	2.5767	1.8115	0.9497	3.3803	0.863
85	ST	15	2	100	3.6765	922.37	10.296	15.792	203.99	2.0766	1.4992	0.7897	2.6829	0.8645
86	ST	5	1	300	3.5526	845.26	6.9809	14.591	230.67	1.3543	1.0133	0.5335	1.7123	0.8683
87	ST	15	2	300	3.6765	864.14	10.964	14.387	205.88	1.8885	1.3456	0.7015	2.4586	0.8704
88	ST	5	2	175	7.8947	918.18	6.2375	20.795	206.22	2.5260	1.7738	0.9311	3.3159	0.8715
89	ST	10	2	100	3.6111	933.15	7.5239	15.569	203.55	2.0110	1.4543	0.7661	2.5957	0.8725
90	ST	5	1	300	7.8947	848.9	10.998	19.375	232.04	2.0067	1.4194	0.7795	2.6233	0.8743
91	ST	15	1	300	3.6765	826.38	12.065	15.37	231.5	1.5066	1.1117	0.5797	1.9215	0.8777
92	ST	10	1	100	3.6111	888.97	8.6863	14.409	228.67	1.7307	1.2782	0.6915	2.206	0.882
93	ST	10	2	175	3.6111	910.54	8.5258	14.737	204.59	1.9883	1.4121	0.7356	2.5934	0.8906

*Source: Binet [11].

pylene pellets and calcium carbonate powder were fed separately by two high-precision gravimetric feeders at the same feed throat location. A slit die instrumented with two 5-MHz ultrasonic sensors, a melt thermocouple, and three pressure transducers, all flush-mounted in the die channel, was used (Fig. 1). The die channel had a 3.0 mm high by 40.0 mm wide rectangular cross-section. The ultrasonic and pressure sensors were installed perpendicular to the 40.0-mm wide surface of the slot. Two ultrasonic sensors were axially aligned, but on the opposite sides of the slot, separately. During measurements, one of the ultrasonic sensors was used as a transmitter to send ultrasonic waves to the molten polymer. The other ultrasonic sensor was used as a receiver. The ultrasonic waves were reflected back and forth several times between the two ultrasonic sensors before completely dying out. By measuring the time delay and amplitude difference between consecutive echoes, the ultrasonic velocity and attenuation coefficient in the molten polymer were obtained [7]. Please note that this instrumented die could be installed at the exit of a variety of extruders.

The experimental data are given in Table 1. These are rearranged data reproduced from an early work carried out at our institute by D. Binet and presented in Ref. 11. The

experiments were designed on a full $2^3 \times 3^1$ factorial plan for 5 levels of filler concentration [12]. The controlled parameters of the process were feeding rate Q_{feed} (2 levels: 3.5 and 7.5 kg/h), screw rotation speed V_{RPM} (3 levels: 100, 175, and 300 rpm), barrel temperature profile T_{prfl} (2 profiles: one, represented by 1 in Table 1, starting at 185°C at the feed throat, with a gradual increase of 5°C from barrel to barrel, up to 225°C at the ninth, with that set-point constant for the remaining barrels and the die; another one, represented by 2 in Table 1, with a constant set-point of 200°C imposed for all sections), the type of filler fed into the extruder F_{type} (2 types: one with stearate coating and denoted as ST in Table 1, and one without coating and denoted as Non_ST in Table 1), and the filler concentration C_f (5 levels: 0, 5, 10, 15, and 20 wt%). The measured parameters are divided into two categories. The first category is extruder-dependent measured variables, which includes the melt pressure profile defined by pressures P_1 , P_2 , and P_3 at three pressure probe locations at the instrumented die shown in Fig. 1, the amperage of electric current A_{mps} required to drive the screws of the extruder. The category of extruder-independent measured variables is composed of variables measured locally at (or near) the ultrasonic probe location. These variables are ultrasonic velocity V_{us} and

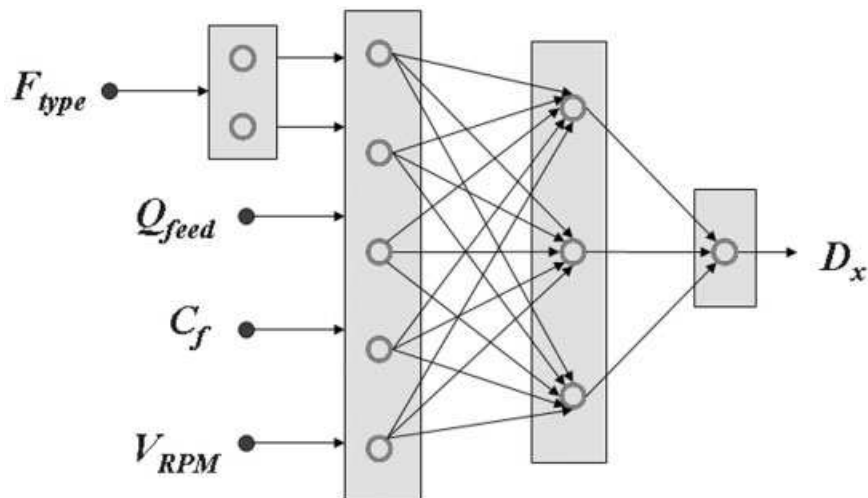


FIG. 2. A four-layer feed-forward network for the estimation of filler dispersion. The network uses only process control variables as inputs.

attenuation coefficient α_{us} in the material being extruded. Since V_{us} and α_{us} measure the mechanical properties of the material and take no account of how the material has been processed, they are extruder-independent variables. It should be pointed out that the sound velocity and attenuation are also functions of melt temperature, pressure. Furthermore, not only the degree of filler dispersion, but also the shear rate, which determines the degree of deformation of polymer chains under flowing condition, can affect the acoustic properties of the polymer. As a consequence, the melt pressure at the ultrasonic probe location P_{us} , the melt temperature T_{melt} read from a melt thermocouple, and the melt shear rate at the ultrasonic probe location $\dot{\gamma}$, should be used with ultrasonic measurement in order to infer filler dispersion state from the ultrasonic data. The shear rate is not easily measurable on-line; however, given the material and the geometry of the melt flow channel of the instrumented die, the shear rate is uniquely determined by the feed rate. This means that the feed rate, Q_{feed} , can be used in place of $\dot{\gamma}$ as an input of the neural network, even though the explicit relationship between the two parameters is unknown. Note that the feed rate Q_{feed} is not only a control variable of the process, but can be a measured variable as well. For the instrumented die used in this work, P_{us} is an extrapolated value of the pressure readings P_1 , P_2 , and P_3 . The parameter of interest to this study was filler dispersion index D_x .

The following definition of the dispersion index, as proposed by Suetsugu [2], was adopted in this study:

$$D_x = 1 - \frac{\Pi}{4A\phi} \sum d_i^2 n_i \quad ,$$

where A is the area of observation, ϕ the volume fraction of filler, d_i the diameter of agglomerates greater than a critical value [2], and n_i the number of agglomerates with diameter

d_i . The best dispersion is obtained when no agglomerate is detected ($D_x = 1$). In the case of worst dispersion, all the particles remain in the form of agglomerates and D_x takes the value of 0. In the present study, the dispersion index was determined through SEM analysis and the critical diameter was set to $7 \mu\text{m}$, which was the upper limit of the diameters of the CaCO_3 particles used in the study. The size of the examined area by SEM was 1.125 by 1.125 mm. Details on laboratory measurements of filler concentration and dispersion can be found in Ref. 12.

ARTIFICIAL NEURAL NETWORK MODELING

Artificial neural network approach is a mapping process that translates a set of measured variables (inputs to the network) into the material property of interest (output of the network). Three network models have been developed for estimating the dispersion index. Except for the inputs, all the networks share the same structure and have the dispersion index D_x as a single output. The first network, shown in Fig. 2, has as inputs only control variables, namely, the filler type F_{type} , the feed rate Q_{feed} , the filler concentration C_f , and the screw speed V_{RPM} . The second network, shown in Fig. 3, has as inputs the filler type F_{type} , the pressures measured at three locations P_1 , P_2 , and P_3 , the melt temperature T_{melt} , the feed rate Q_{feed} , and the amperage A_{mps} . In the third network, shown in Fig. 4, we want to use the ultrasonic velocity V_{us} and attenuation coefficient α_{us} to infer the dispersion index. Note that both V_{us} and α_{us} are not only functions of the state of filler dispersion, but also functions of melt pressure, temperature, and shear rate (which is determined by the feed rate for a given material and die geometry). As a consequence, the melt temperature T_{melt} , the melt pressure at the ultrasonic probe location P_{us} , and the feed rate Q_{feed} are used as inputs of the network as well.

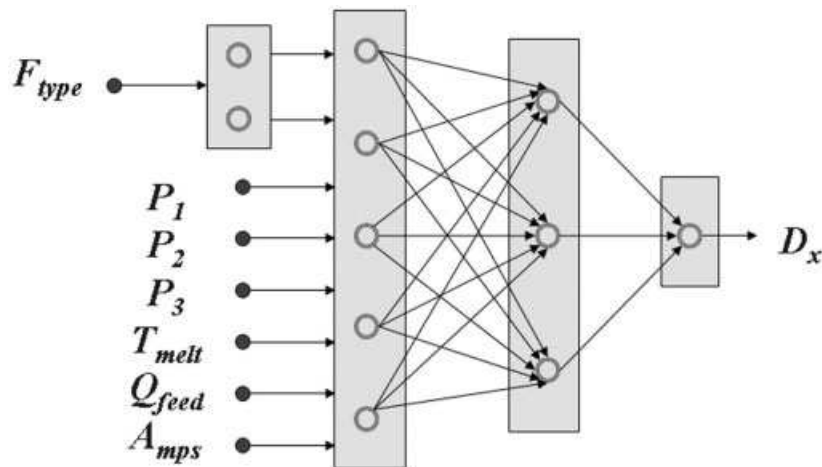


FIG. 3. A four-layer feed-forward network for the estimation of filler dispersion. No ultrasonically measured variables are used as inputs.

Table 2 shows the correlations between some of the variables listed in Table 1 and the dispersion index D_x . As can be seen in Table 2, the ultrasonic velocity, V_{us} , is practically not correlated to the dispersion index. However, we still use V_{us} as one of the inputs of the third neural network. This is because the ultrasonic velocity is particularly sensitive to the thermal degradation (determined by polymer thermal history during the process) of the polymer [13] and the polymer degradation can also affect the ultrasonic attenuation α_{us} . As a matter of fact, V_{us} and α_{us} are physically interrelated. From Table 1, the correlation coefficient between V_{us} and α_{us} is calculated as -0.54 , which is much more significant than the value of 0.009 between V_{us} and D_x . Introducing V_{us} in the network model can help reduce the influence of thermal history on the estimation of distribution index.

Our analysis of Table 1 has shown that the surface

condition, i.e., with or without stearate coating, of fillers, has strong effects on the quality of dispersion. More precisely, under similar processing conditions, the coated filler performed consistently better than the noncoated one in terms of dispersion index. Therefore, the filler type F_{type} was used as an input to all of the three networks. The filler type was coded as 1 for the stearate-coated filler and 2 for the noncoated filler. Obviously, the effects of the two filler types on the process could not be represented with these two rather arbitrarily chosen simple values. We used a two-neuron layer to represent the effect of the filler type. With this layer, each filler type was characterized by two output numbers of which the values were to be determined by the network training process.

The neural networks were implemented using a commercial MATLAB® Neural Network Toolbox. The networks used a hyperbolic tangent sigmoid transfer function for the

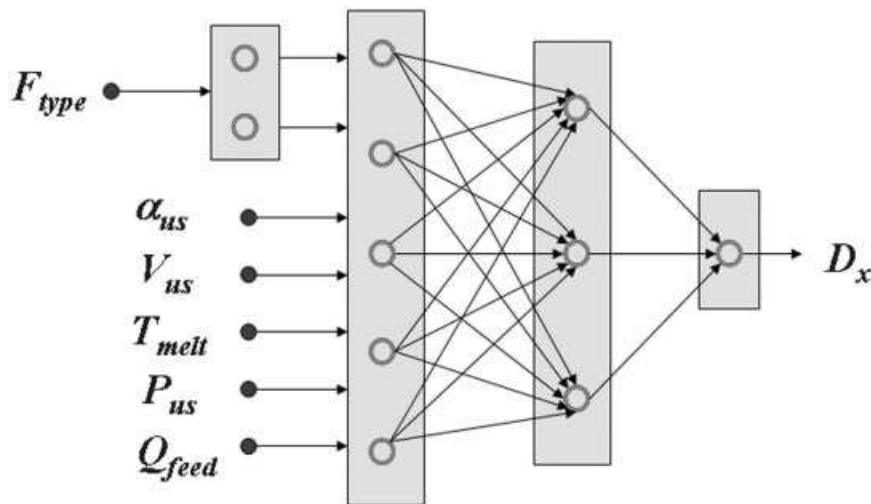


FIG. 4. A four-layer feed-forward network for the estimation of filler dispersion based on ultrasonic attenuation and velocity measurement.

TABLE 2. Correlation coefficients between variables listed in Table 1 and the dispersion index.

Variables	C_f	V_{RPM}	Q_{feed}	V_{us}	α_{us}	A_{mps}	T_{melt}	P_1	P_2	P_3	P_{us}
Correlation coefficient	-0.13	0.22	-0.57	0.009	-0.39	-0.65	-0.29	-0.54	-0.48	-0.51	-0.56

neurons (i.e., processing unit) at the hidden layers, and a linear transfer function for the output layer. However, only the first hidden layer had a bias connection. The weight factor associated with each interconnection between an input and a neuron or between two neurons as well as the biases of the first layer were adjusted (in other words, the networks were trained) according to Levenberg-Marquardt back-propagation optimization. To overcome the overfitting problem inherent to the back-propagation algorithm, we utilized a validation data set and an early stopping strategy by which the training stopped after a minimal mean squared error of the network output with respect to the validation data had been achieved.

Of the available 93 dispersion index measurements (47 for stearate-coated filler and 46 for noncoated filler), 47 were chosen to form a data set for network training, and the rest were used to form a validation-testing data set. Because of the limited number of samples, for each training, one-half of the data samples were chosen randomly from the validation-testing data pool to form a validation data set, and the remaining data for the testing data set. A total of 30 pairs of thusly-formed data sets were used in the training process, resulting in 30 trained networks. Each of the 30 trained networks was the best result of trainings for 1000 different initial weight and bias conditions. The best result was defined as the one with the smallest maximum error on the 93 estimated D_x compared with the measured ones. Among the 93 estimates of D_x , 47 were from training, 23 from validation, and 23 from testing. A comparison of the 30 trained networks allowed us to evaluate the robustness of the network models.

RESULTS AND DISCUSSIONS

Table 3 shows the errors on the estimates of the dispersion indices generated by the networks depicted in Figs. 2,

TABLE 3. Errors on the estimates of dispersion indices generated by three neural networks.

Neural network models	ϵ_{max_mean}	ϵ_{rms_mean}	ϵ_{max_best5}
Network with process control variables as inputs (Fig. 2)			
Temperature profile 1	0.0527	0.0117	0.0456
Temperature profile 2	0.0363	0.0093	0.0323
Network with extruder-dependent non-ultrasonically measured variables as inputs (Fig. 3)	0.0631	0.0141	0.0548
Network with extruder-independent ultrasonically measured variables as inputs (Fig. 4)	0.0595	0.0127	0.0487

3, and 4, respectively. In Table 3, ϵ_{max_mean} represents the average of the maximum errors generated by the 30 trained networks, ϵ_{rms_mean} the average of the root-mean-square errors of the estimates produced by the 30 trained networks with regard to the measured values of the samples, and ϵ_{max_best5} the maximum of the errors generated by the average of the estimates provided by the five best trained of the 30 networks compared with the measured dispersion indices. In this work, we used the average of the estimates provided by the five best trained of the 30 networks as the final estimate produced by the model. For the network of Fig. 2, where only the control parameters were used as inputs, the estimation error ϵ_{max_best5} on dispersion index was less than 0.033 on a scale of 0 to 1 for the case in which a constant set point of 200°C was imposed for all barrel sections. This error was less than 0.046 for the case where the temperature profile of the extruder barrel temperature was set at 185°C at the feed throat, with a gradual increase of 5°C from barrel to barrel up to 225°C at the ninth, and at 225°C for the remaining barrels and the die. Given that even the SEM utilized in this study had a 10% chance of producing an error of larger than 0.05 on dispersion index measurement (of course these errors were mostly filtered out in the averaged data used in this study), the performance of this network is excellent. Deviations of estimated dispersion indices, produced by the present as well the other networks presented in this work, from the measured ones could result from insufficient data size in the network training, and the network structure that may not reproduce the exact process. The instability of the process itself, discrepancy between the readings and the real values of the process and measured variables, limited accuracy on dispersion index measurement, could also result in deviations of the network estimates from the measured results. The excellent prediction of the dispersion index through application of the control variables of the process to the network suggests a deterministic nature of the dependency of the state of filler dispersion on the operating conditions of the extrusion process. The neural network model established could be used as a simulation tool to determine the optimal process conditions to achieve a desired and practically achievable dispersion quality. However, since the effects of a given process control condition depends largely on the status and configuration of the screws and barrel, the neural network model based on control variables is extruder-dependent. In other words, for the model to be valid, it has to be retrained upon every change made to the screw and barrel. This obviously limits the usefulness of such a model.

The neural network of Fig. 3 has generated an estimation error of less than 0.055 and can be considered good as well.

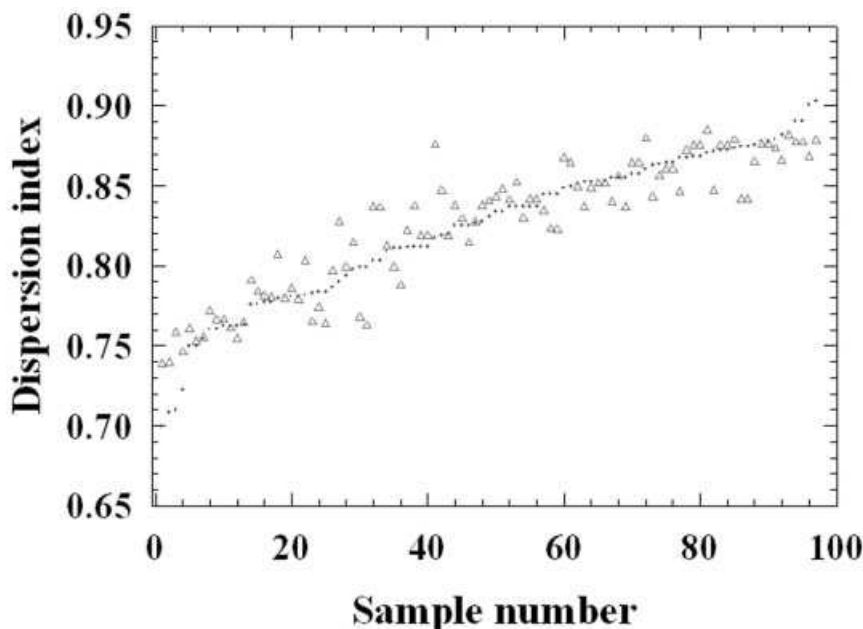


FIG. 5. Comparison between measured (dots) and the average of 5 estimated dispersion indices produced by 5 best-performed networks (triangles).

This shows that the filler dispersion can be monitored reasonably well even without using ultrasound. However, since this network uses pressure profile in the melt channel as well as the amperage as inputs, and the pressure profile and amperage are determined by the status and configuration of the screw and barrel, this neural network model is also extruder-dependent. This means that the model is not transportable from one extruder to another, and it has to be recalibrated upon every change made to the screw and barrel. This calibration will require new experiments on the modified extruder and new SEM analysis of extrudates in order to establish a relationship between those measured input variables of the neural network and the quality of dispersion.

The neural network model depicted in Fig. 4 has produced excellent estimates on dispersion indices, with an estimation error of less than 0.049. Figure 5 shows a comparison between the estimated dispersion index generated by the neural network model of Fig. 4 and those measured with SEM. This network has produced better results than those provided by the non-ultrasonic measurements shown in Fig. 3. This suggests that ultrasonic measurement is more sensitive to the state of dispersion than the pressure and amperage measurements. In fact, unlike the ultrasonic measurement, the pressure and amperage can only provide information on process conditions which dictate the final state of the filler dispersion rather than measuring directly the state of filler dispersion itself. Since all the inputs of the ultrasonic network model shown in Fig. 4 are related solely to the status of the melt at the probed location, this model is extruder-independent and transportable to other extruders of the same or different types and sizes. The transportability is the most important feature of the ultrasonics-based models.

Since the establishment of these models require large amount of calibration work, the transportability means enormous savings of resources in the future for model development once the models have been successfully established and this makes the models practically useful for in-line monitoring of filled-polymer extrusion processes. However, it should be pointed out that, like any expert or database systems, the neural networks do not generate more knowledge than what they received during training. In order to apply neural networks successfully, the user has to make sure that the input variables fall in the ranges in which the networks have been trained. It is also important to remember that the network is valid only for the material system for which it has been trained, although the approach could be generalized to other material systems.

CONCLUSION

In this work, three artificial neural networks have been established and tested for the determination of the dispersion of calcium carbonate powder in a polypropylene matrix. Among the three networks, one uses process control variables as inputs, one uses extruder-dependent measured variables as inputs, and the remaining one uses ultrasonic measurement data as well as other extruder-independent measured variables as inputs. All of the three networks performed well in the estimation of filler dispersion index. However, neural network models with ultrasonic measurement data as inputs are most promising for in-line monitoring of filler dispersion owing to their transportability. This study has demonstrated the feasibility of using ultrasound and neural networks together for in-line monitoring of dis-

persion during extrusion processes of mineral-charged polymers.

REFERENCES

1. B.M. Mutagahywa and D.A. Hemsley, *Plast. Rubb. Process. Appl.*, **5**, 219 (1985).
2. Y. Suetsugu, *Int. Polym. Process.*, **V**, 184 (1990).
3. L. Avérous, J.-C. Quantin, and A. Crespy, *Compos. Sci. Technol.*, **58**, 377 (1999).
4. M. Appello, *Plast. Rubb. Compos.*, **29**, 207 (2000).
5. P.P. Sukhanov, A.E. Zaikin, and V.S. Minkin, *Int. Polym. Sci. Technol.*, **16**, T15 (1989).
6. S. Okuda and K. Fujisawa, *Proc. Mech. Behav. Mater.—Conference VI*, Kyoto, Japan, 671 (1991).
7. R. Gendron, L.E. Daigneault, J. Tatibouët, and M.M. Dumoulin, *Adv. Polym. Tech.*, **15**, 111 (1996).
8. Z. Sun, C.-K. Jen, C.-K. Shih, and D. Denelsbeck, *Polym. Eng. Sci.*, **43**, 102 (2003).
9. J. Tatibouët and M.A. Huneault, *Int. Polym. Process.*, **XVII**, 49 (2002).
10. S. Haykin, *Neural Networks: A Comprehensive Foundation*, 2nd ed., Prentice Hall, Upper Saddle River, NJ (1999).
11. D. Binet, “Quantification de la dispersion d’une charge minérale et d’un polymère extrudés par les réseaux de neurones,” Master’s thesis, Univ. Sherbrooke (Quebec), Canada (1996).
12. R. Gendron and D. Binet, *J. Vinyl Addit. Technol.*, **4**, 54 (1998).
13. J. Tatibouët, A. Hamel, and L. Piché, *Proc. Polym. Process. Soc. 15th Annual Meeting*, s’Hertogenbosch, The Netherlands (1999).